Plant Systematics and Evolution (2020) 306:39
https://doi.org/10.1007/s00606-020-01666-8

ORIGINAL ARTICLE

Allopolyploidy and genomic differentiation in holocentric species of the *Eleocharis montana* complex (Cyperaceae)

Lucas Johnen[1] · Thaíssa B. de Souza[1] · Danilo M. Rocha[1] · Letícia M. Parteka[1] · Maria S. González-Elizondo[2] · Rafael Trevisan[3] · Srinivasa R. Chaluvadi[4] · Jeffrey L. Bennetzen[4] · André L. L. Vanzela[1]

Received: 6 September 2019 / Accepted: 20 February 2020 / Published online: 17 March 2020

Abstract

Polyploidy and hybridization are key events in plant evolution. Due to these events, complexes of species can be formed. Dysploidy, a frequent chromosome change in holocentric organisms, may add some difficulties to species delimitation, especially in Cyperaceae. The *Eleocharis montana* complex is known for its members with overlapping morpho-anatomical features and unclear circumscription. To understand its biological history, several tools were used to investigate different American populations, including morpho-anatomical analysis, genome size estimates, cytogenomic analysis, molecular marker characterization, and genomic in situ hybridization (GISH). Despite overlapping morphological features, it was possible to separate two groups, the first containing *E. parodii* and *E. subarticulata*, presenting diploid and dysploid karyotypes, respectively, and small DNA C-values. The second contained *E. elegans*, *E. contracta,* and *E. montana*, with large genomes created by polyploidy. All analyses suggest that *E. montana* with $2n = 40$ is a cytotype of *E. contracta* with $2n = 20$, and both evolved from a natural hybridization involving *E. parodii* ($2n = 10$) and a second progenitor that is yet unknown. Furthermore, the GISH results indicated that *E. parodii* may be an ancestor of *E. elegans.* All species occur in the probable center of diversification in Austral South America, where the hybridization zone is identified. Fieldwork and information obtained from herbaria indicate that diploid and dysploid species (*E. subarticulata* and *E. parodii*) do not occur beyond the center of diversification. However, *E. elegans* and specially *E. montana* occur more widely, occupying different flooded environments and landscapes.

Keywords Cytogenomic analysis · GISH · Holocentric chromosomes · Hybridization · Molecular markers · Polyploidy

Introduction

Polyploidy is an important mechanism of plant evolution. There are two main polyploid types, autopolyploidy, which arises from the genomic duplication of one species, and allopolyploidy, which arises from the duplication of hybrid genomes (del Pozo and Ramirez-Parra 2015). In general, allopolyploids present overlapping morphological and genomic features in relation to progenitors, as well as higher vigor, invasiveness, and adaptation to different habitats (Whitney et al. 2010; Dar et al. 2017). However, allopolyploid recognition can be difficult due to the lack of morphological characteristics indicative of the hybridization processes and the low frequency of progenitors in the hybrid zone or progenitor extinction (Queiroz 2007; Soltis and Soltis 2009; Kerbs et al. 2017).

Although polyploidy plays an important role in Cyperaceae (sedge) evolutionary history, the occurrence of

Handling Editor: Martin A. Lysak.

Electronic supplementary material The online version of this article (https://doi.org/10.1007/s00606-020-01666-8) contains supplementary material, which is available to authorized users.

✉ André L. L. Vanzela
andrevanzela@uel.br

[1] Laboratory of Cytogenetics and Plant Diversity, Department of General Biology, Center for Biological Sciences, State University of Londrina, Londrina, Paraná 86057-970, Brazil

[2] CIIDIR, Instituto Politécnico Nacional, Sigma 119 Fraccionamiento 20 de Noviembre II, 34220 Durango, Mexico

[3] Department of Botany, Federal University of Santa Catarina, Florianópolis, Santa Catarina 88010-970, Brazil

[4] Department of Genetics, University of Georgia, Athens, GA 30602-7223, USA

chromosomal fissions and fusions is believed to be favored in sedges, due to the presence of holocentric chromosomes (Luceño and Guerra 1996; Bureš and Zedek 2014; Yano et al. 2016; Da Silva et al. 2005, 2017). According to Ribeiro et al. (2018), the combination of polyploidization with dysploidy is frequent in species with holocentric chromosomes, and it has been suggested for a few species of *Carex* L. (Catling et al. 1989; Escudero et al. 2018), *Schoenoplectus* (Rchb.) Palla (Fay et al. 2003), *Scirpus* L. (Yang et al. 2009), and *Eleocharis* R.Br. (Da Silva et al. 2017).

The genus *Eleocharis* includes ~ 250 species (Yano et al. 2004; Roalson et al. 2010; Hinchliff et al. 2010) recognized by the absence of leaf blades, unbranched culms with basal sheaths, and a single terminal spikelet per culm (Goetghebeur 1998). The clade named "*Eleocharis montana* complex" (Roalson et al. 2010) includes species with overlapping morphological characters, some identification conflicts and wide genome diversity. Five species occur in southern South America (*E. parodii* Barros, *E. subarticulata* Boeckeler, *E. contracta* Maury, *E. elegans* Roem. & Schult., and *E. montana* Roem. & Schult.); the last two species extend into southern North America, with sympatry occurring between *E. ravenelli* Britton in Small and *E. densa* Benth. (see González-Elizondo and Tena-Flores 2000; Da Silva et al. 2005, 2010; WCSP: World Checklist of Selected Plant Families 2014). The *E. montana* complex exhibits a restricted distribution for diploid and dysploid species and a broad radiation of polyploids in the American continents. Although the phylogenetic resolution was clear for this clade (Roalson et al. 2010), there are doubts about the role of hybridization and polyploidy in the karyotype differentiation of this group containing holocentric chromosomes.

In the last decades, molecular systematics has been a powerful tool to resolve phylogenetic relations in a variety of plant groups. However, hybridization and polyploidy events may create a "discontinuity" among species, which makes it difficult to establish some relationships based only on molecular markers (Fazekas et al. 2009). The *Eleocharis montana* complex is a good example, as it has a broad radiation of polyploids in the American continent, with cases of discontinuity or overlapping of morphological characters, associated with polyploidy and dysploidy. These events can be related to the lack of resolution between clade members, especially when molecular phylogeny is used (see Roalson et al. 2010). Given this, our main question was: What was the process of polyploid evolution in this complex?

Species in the *E. montana* complex, especially *E. montana* itself, are of interest for being invasive perennial herbs, occupying the most diverse types of humid and degraded environments. The combined use of morphological, anatomical, cytological, genomic, and molecular tools can be a good strategy to elucidate the interspecific and intraspecific relationships in this clade. In order to understand the biological history of this holocentric group that occurs across the Americas, different species and populations were compared. Discussion considers the probable center for diversification and speciation, and the genomic differentiation processes based on the hybridization and polyploidy.

Materials and methods

Biological sampling

One hundred and eleven (111) individuals of the *Eleocharis montana* complex, including *E. parodii* (3), *E. subarticulata* (9), *E. elegans* (4), *E. contracta* (3), and *E. montana* (92), were collected from different populations, landscapes, and environments along the South, Southeast, and Midwest regions of Brazil. Except *E. montana*, which is very common in many degraded and flooded environments, the other species are rarely found. Because of this, there are a limited number of samples for some species. Collection details can be viewed in Online Resources 1 and 2. Vouchers of *E. montana, E. contracta*, *E. elegans*, *E. subarticulata*, and *E. parodii* were deposited and analyzed in the herbaria FUEL (Londrina, PR, Brazil) and FLOR (Florianópolis, SC, Brazil). Samples were grown in the greenhouse of the Laboratory of Cytogenetics and Plant Diversity of State University of Londrina, Brazil.

Morphological and anatomical analyses

Although the circumscription of the *E. montana* complex is well established for most species, there are still doubts about the relationship between *E. montana* and *E. contracta*. To support our hypothesis of evolution through hybridization and polyploidy, we also performed a morpho-anatomical comparison in all South American species of this complex. The morphology of the culms, sheath, glumes, inflorescences, and achenes were compared according to Trevisan (2009). For this, images were acquired using a S6D stereomicroscope coupled with an EC3 camera, both Leica. Measurements were taken with a ruler, of scale 0.5 mm, adequate to the GIMP 2.8 program. Mean values, standard deviation, and variance were calculated in the LibreOffice Calc program. In order to separate the species and populations by achene shape, additional analyses were performed, considering the transversal section of the achenes. Principal component values (PC1, PC2, and PC3) were obtained on the perimeter, area, and shape of the achene structures, using 50 achenes per species. Images were treated and compared using the LeafAnalyser 2.3.0 program, with 48 selected landmarks, considering the orientation of achenes (from base to apex of the stylopodium).

For the anatomical analyses of culms, thin sections were obtained from the median region of fresh culms containing mature inflorescences using disposable steel razor blades. Sections were stained in toluidine blue (0.05% in phosphate buffer pH 6.8) and afterward washed and mounted on glass slides using distilled water. In addition to hand sectioning, some culms sections were obtained from materials fixed, processed, and blocked in hydroxyethylmethacrylate (Gerrits and Smid 1983). Thin sections (5 µm) were made using a rotating microtome, stained with toluidine blue (0.05% in phosphate buffer pH 6.8) and mounted on glass slides using Entellan (Merck). Samples were observed in a Leica DM4500B light microscope and photographed with a Leica DFC300FX camera. The obtained images were edited for optimal brightness and contrast in GIMP 2.8, Linux.

In addition to these analyses, all diagnostic features were used to compose a matrix in the Mesquite program (https://www.mesquiteproject.org). The analyses were performed using clustering UPGMA from absolute distance of character matrix, with the default parameters of Mesquite.

Genome sizes estimates and conventional cytogenetics

Measurements of the DNA C-values were taken using the young culms fragmented using a sharp razor blade in 125 µL of the Otto I buffer, containing 22 µL of polyethylene glycol 4000 (40%) and 6 µL of RNase (1 mg/mL), later treated with 125 µL of Otto I buffer for 2 min. Samples were filtered in a 25 µm nylon mesh, centrifuged at 100 g for 5 min, and stained using a solution composed of 90 µL of Otto I, 180 µL of Otto II, 65 µL of polyethylene glycol 4000 (40%), 19 µL of 1 mg/mL RNase, and 19 µL of propidium iodide (1 mg/mL) for 40 min (Doležel et al. 2007). The readings were performed on a BD ACCURI C6 flow cytometer, in three independent estimations on different days. *Solanum lycopersicum* "Stupické polní rané" ($2C = 1.96$ pg) was used as an internal standard. The $2C$ values were calculated using at least 30,000 nuclei for each species (CV < 5%), estimating the sample peak mean/standard peak means × $2C$ DNA amount of standard (pg). Analyses of variance (ANOVA) were performed using the Sisvar 5.6 program, using the hypothetical monoploid complement (Cx) values per sample. The means comparison (Tukey's HSD, < 5%) and Pearson correlation tests were performed in R (/www.r-project.org), and the graphs were elaborated with the Gnumeric 1.12.9 program.

Mitotic chromosomes were obtained from root tips treated with 2 mM 8-hydroxyquinoline for 24 h and fixed in a fresh solution of ethanol/acetic acid (3:1, v:v) for 24 h. Samples were softened in 2% cellulase and 20% pectinase (w/v) at 37 °C for 1 h, hydrolyzed in 1 M HCl for 10 min at 60 °C, and squashed in a drop of 60% acetic acid. Slides were stained in 2% Giemsa and mounted with Entellan (Merck). The chromosome counts were performed in at least ten cells for each sample. The images were acquired using a DM4500B microscope with a DFC300FX camera, both Leica.

Genomic analysis and molecular markers

Nuclear DNA was isolated from the young culms of *E. parodii* seedlings (3 samples), *E. subarticulata* (5 samples), *E. elegans* (3 samples), *E. contracta* (3 samples), and *E. montana* (16 samples). DNA was obtained using 2% cetyltrimethylammonium bromide (CTAB) extraction buffer (Doyle and Doyle 1987), purified with phenol/chloroform (1:1, v/v), chloroform/isoamyl alcohol (24:1, v/v), and RNase (1 mg mL^{-1}), and then precipitated in 100% absolute ethanol. After resuspension in Tris–HCl pH 8.0, the samples were tested in 1% agarose gel using a NanoDrop 2000 Spectrophotometer (Thermo Scientific).

The genomes were compared using two markers: (i) inter-simple sequence repeat (ISSR) and (ii) retrotransposon-microsatellite amplified polymorphism (REMAP). The genomes of *E. parodii*, *E. elegans,* and *E. montana* were sequenced using Illumina Miseq PE250; the reads were deposited in the NCBI database, as NCBI: SRR9313477, SRR6144762, and SRR9313478, respectively. The assemblies were performed with the SPAdes program using three K-mers (31, 51, and 71) concomitantly. The scaffolds were compared according to the occurrence and diversity of transposable elements (TEs), using conserved protein domains deposited on the RepBase (girinst.org/censor/), *Gypsy*DB (gydb.org/index.php/MainPage), and NCBI (ncbi.nlm.nih.gov/) databases. Sequences were organized according to classes, superfamilies, and families (Llorens et al. 2009): Class 1 LTR-RTs: *Gypsy* (Reina, Galadriel, Del, CRM, Athila, and Tat) and *Copia* (Oryco, Retrofit, SIRE, and Tork) and Class 2 transposons: CACTA, Mutator, Harbinger, hAT, and Helitrons. Microsatellite (SSR, Simple Sequence Repeats) frequency was estimated using the SSRIT script (Simple Sequence Repeat Identification Tool) (http://archive.gramene.org/db/markers/ssrtool), edited and organized to consider two to six Mers motifs. The GA_9 oligomer was applied to the ISSR (Inter-Simple Sequence Repeats) reaction. Two forward primers representing the conserved reverse transcriptase region of *Gypsy*-DEL (5' GCCGGG CCATTAGTATTTT) and of *Copia*-Oryco (5' GCTCAA GAGGCACTTCTGGT) retrotransposons were selected and used for REMAP (retrotransposon-microsatellite amplified polymorphism), in separated reactions with GA_9 used as the reverse primer.

For the ISSR and REMAP analyses, reactions contained a mix of 25 µL composed of 10 mM dNTP (1 µL), 5 mM

of each primer (2 µL), 50 mM $MgCl_2$ (1.5 µL), 10× buffer (2.5 µL), 2.5 U of Taq polymerize (0.5 µL), 10 ng template (5 µL), and ultra-pure water (12.5 µL). Reactions for ISSR and REMAP were performed in a PTC-100 Thermal Cycler (BioRad, Foster City, CA, USA) programmed to 94 °C for 2 min, 30 cycles of 94 °C for 40 s, 60 °C for 40 s, and 72 °C for 1 min and a final extension at 72 °C for 10 min, according to Kalendar and Schulman (2006), with modifications. Reactions were tested using electrophoresis in an agarose gel at 3 V cm^{-1} and stained with ethidium bromide.

The PCR fragments from 30 populations, including 105 landmarks, were analyzed as binary characters (0 and 1), and data analyses were performed using the Jaccard coefficient to generate a distance matrix. This genetic matrix was employed to elaborate a dendrogram by the UPGMA method (Unweighted Pairwise Group Method using Arithmetic Average). All analyses were carried out using the online http://insilico.ehu.es/dice_upgma/ tool. The dendrogram was edited in Figtree 1.4.2. (Rambaut 2007).

Phylogeny approach based on rDNA and chloroplast sequences

In order to enrich the molecular analysis, rDNA and chloroplast sequences (Online Resource 3) were used in two ways, with independent and concatenated matrices. In the first case, sequences were analyzed using the following routine: (i) MUSCLE alignment (bootstrap 500); (ii) verification of alignment with Gblocks; (iii) phylogenetic tree organization based on maximum likelihood using PhyML and Bayesian inference using MrBayes; and (iv) TreeDyn rendering (http://www.phylogeny.fr/index.cgi). Dendrograms were edited in Figtree 1.4.2. (Rambaut 2007). Additionally, sequences were used to organize independent matrices, which were concatenated in the Mesquite program. Data were analyzed using clustering via UPGMA from absolute distance of character matrix, with default parameters of Mesquite.

Genomic in situ hybridizations (GISH)

Genomic DNA of all species was extracted and purified using CTAB, as previously described (Doyle and Doyle 1987). Samples (~2 µg of DNA) were denatured at 120 °C and 1.2 atm for 5 min to obtain ~1000-bp length fragments. DNA was labeled with biotin-14-dATP using nick translation. The probes from all genomes were tested against all karyotypes, in slides prepared using squashed material, without acid hydrolysis. For each GISH reaction, a mix containing a solution (30 µL) composed of 100% formamide (15 µL), 50% polyethylene glycol (6 µL), 20× saline-sodium citrate (SSC; 3 µL), 10% sodium dodecyl sulfate (SDS; 1 µL), and 100-ng probes (5 µL) was used. The mix was denatured at 90 °C for 10 min. Hybridization was performed at 37 °C for 24 h. Post-hybridization washes were performed using 70% stringency with an SSC buffer, pH 7.0. After probe detection with the avidin-FITC conjugate, washes were performed twice in 4× SSC/0.2% Tween 20 at room temperature. Slides were mounted with 25 µL of a solution composed of glycerol (90%), DABCO (2.3%), 20 mM Tris–HCl (tris(hydroxymethyl)aminomethane), pH 8.0 (2%), 2.5 mM $MgCl_2$ (4%), and distilled water (1.7%), in addition to 1 µL of 2 mg mL^{-1} DAPI.

Results

Morpho-anatomical approach

Given the great similarity between the smaller forms of *E. montana* and *E. contracta*, we performed a broader comparative analysis with samples of these two species, as well as with all others in the complex (Table 1). The culms varied from spongy to irregularly septate, with mucronated sheaths, except in *E. subarticulata* (Fig. 1a–e). The spikelets were lanceolate with 30–50 flowers, cylindrical with

Table 1 Morphological feature variation in the species of the *Eleocharis montana* complex

	E. parodii	*E. subarticulata*	*E. elegans*	*E. contracta*	*E. montana*
Culm	Spongy	Spongy	Septate	Septate	Septate
Sheat	Slightly oblique	Oblique	Truncate	Truncate	Truncate
Apex sheat	Mucronate	With dorsal mucro	With dorsal mucro	With dorsal mucro	With dorsal mucro
Spikelet	Lanceoloid	Cylindrical	Lanceoloid	Lanceoloid	Lanceoloid
Number of flowers	30–50	400–800	500–700	20–150	20–400
Floral scale	Membranous	Membranous	Membranous	Membranous	Membranous
Floral scale shapes	Ovate/obovate/ovate-lanceolate	Ovate/obovate/ovate-lanceolate	Oval	Ovate/obovate/ovate-lanceolate	Ovate/obovate/ovate-lanceolate
Floral scale apex	Obtuse–apiculate	Acute	Acute–obtuse	Acute–obtuse	Obtuse–apiculate
Achene	Trigonous	Trigonous	Trigonous	Biconvexos/trigonous	Biconvexos/trigonous
Stylopodium	Pyramidal	Pyramidal elongated	Pyramidal	Pyramidal/flattened dorsiventrally	Pyramidal/flattened dorsiventrally

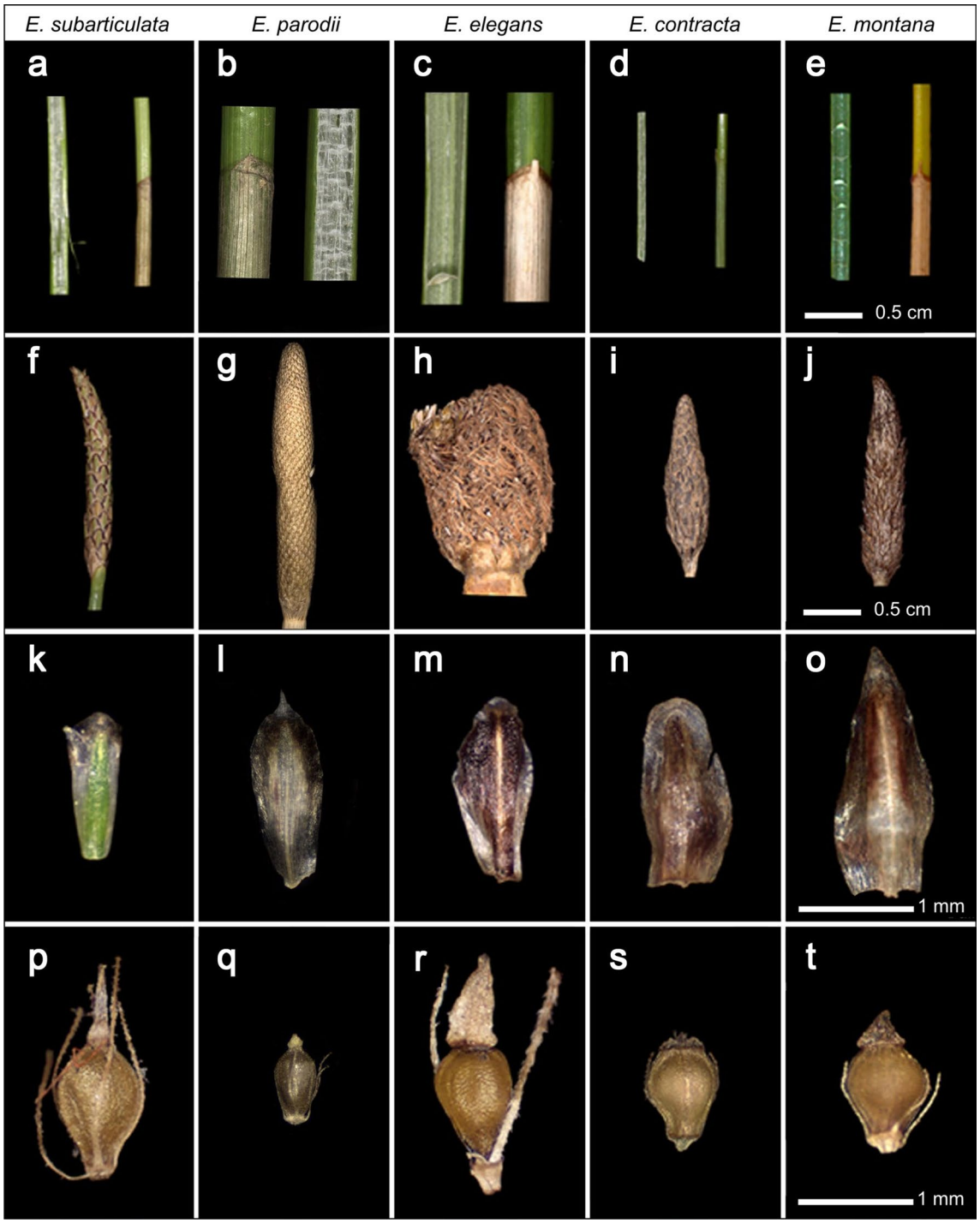

Fig. 1 Comparison of morphological details on the species of the *Eleocharis montana* complex from southeastern and southern Brazil. The culms (**a**–**e**) exhibited a variable profile, being septate in *E. elegans*, *E. contracta*, and *E. montana*, while being spongy in *E. subarticulata* and *E. parodii*. The spikelets (**f**–**j**) vary in size and the number of flowers. The glumes (**k**–**o**) differ in all species, although there exists some overlap between *E. montana* and *E. contracta*. The achenes (**p**–**t**) have evident differences in the size and shape of stylopodia, being the scales of *E. parodii* in the apiculated apex, contrary to others, which are acute to obtuse

400–800 flowers, and oval to lanceolate with 20–400 flowers (Fig. 1f–j), with glumes ranging from oval to ovate-lanceolate (Fig. 1k–o). Achenes were olivaceous to dark brown, biconvex to trigonous, ~ 0.8 mm to ~ 2 mm long, with evident differences in the size and shape of stylopodia, which are pyramidal (Fig. 1q, s, t) to lanceolate in their outline, but

dorsiventrally flattened (Fig. 1p, r). The comparative analysis using the shape and size of achenes between samples of *E. montana* and *E. contracta* (the two more closely related species) showed a large variation in size, flattened shape, and the stylopodia apex among species, especially between the samples of *E. montana* that are commonly larger than those of *E. contracta* (Online Resource 4). However, the smaller forms of *E. montana* may be very easily confused in the field with *E. contracta*.

Moreover, the principal component analysis (PCA) showed three groups of fruit morphologies. One was represented by *E. parodii*, which exhibited a reduced size, including stylopodium, and an evident narrowing at the achene apex (Fig. 1q and Online Resource 4). The second group included *E. contracta* and *E. montana* (Fig. 1s, t and Online Resource 4) with a pyramidal stylopodium, shorter hypogonous setae not longer than the achene body, which is biconvex to trigonous. The third was comprised of *E. elegans* and *E. subarticulata*, exhibiting a lanceolate to narrowly pyramidal stylopodium with a thin base, and hypogynous setae longer than the achene body, exhibiting a trigonous shape (Fig. 1p, r, respectively, and Online Resource 4). The comparison of morphological features using a distance matrix by the UPGMA method formed two groups, one with *E. elegans* and *E. montana*, and *E. contracta* positioned at the base, and the second with *E. parodii* and *E. subarticulata* (Online Resource 5).

The specimens of *E. montana* varied in the sizes of all morphological characters (Online Resource 6 and Fig. 2a–z), and the smaller representatives were very similar to *E. contracta*. Culms ranged from 0.97 to 1.73 mm in diameter, with septa arranged irregularly and sheaths always mucronate (Fig. 2a–j). Spikelets varied from 5 to 21 mm (Online Resource 6 and Fig. 2k–o), some being smaller than those of *E. contracta* but never larger than those of *E. elegans* (Fig. 1). These were ovoid to lanceolate, depending on the size; however, in general, they were usually lanceolate (Fig. 2k–o). The scales exhibited a very thin hyaline margin, well delimited and with the apex being acuminate to acute (Fig. 2p–t). The achenes of *E. montana* exhibited olivaceous to dark brown staining, maintaining the biconvex form of the trigone (Fig. 2u–z).

Culm anatomy was relatively similar among these species. The epidermis appeared uniseriate; underneath it, the chlorophyllic parenchyma was present, containing one to three layers of paliçadic cells (Fig. 3). The culms, however, were mostly made of aerenchymatous tissue. In *E. montana, E. contracta*, and *E. elegans*, this aerenchyma exhibited regular lacunes between the vascular bundles and a large central cavity was observed (Fig. 3a–d). In *E. subarticulata* and *E. parodii*, the aerenchyma was very pronounced but presented irregular lacunes, without the formation of a large central cavity (Fig. 3e, f). Only *E. parodii* presented stellate parenchyma underneath the chlorenchyma (Online Resource 7), observed exclusively in freehand sectioning (Fig. 3f).

DNA C-value comparisons versus karyotype features

The DNA amount (2*C*) estimates showed a range from 1.570 pg in *E. subarticulata* ($2n = 2x = 6$) and 1.574 pg in *E. parodii* ($2n = 2x = 10$) to 4.800 pg in *E. montana* ($2n = 8x = 40$), with the hypothetical monoploid values (C*x*) variation from 0.553 pg in *E. elegans* ($2n = 4x = 20$) to 0.787 pg in *E. parodii* (see the complete results in Table 2 and Fig. 4a). The ANOVA analysis demonstrated significant differences of $F_{3.48} = 2068$ ($p < 000.1$) to 2*C* and $F_{3.48} = 176.1$ ($p < 000.1$) to C*x*. In both cases, Tukey's test confirmed a significant variation ($p < 0.05$), except to *E. subarticulata* and *E. parodii* ($p = 0.99$). It is thus important to highlight that $2n = 6$ of *E. subarticulata* (Fig. 4b) arose after symploidy while $2n = 10$ of *E. parodii* (Fig. 4c) follows the chromosome base number of subgenus *Eleocharis.* The karyotypes with $2n = 20$ of *E. contracta* and *E. elegans* (Fig. 4d, e), and $2n = 40$ in *E. montana* (Fig. 4f), are polyploid. The flow cytometry data showed a positive correlation between a higher DNA C-value and ploidy levels, with $R^2 = 0.83$ for 2*C*, but with a slight decrease in C*x* values in relation to increasing ploidy, with $R^2 = 0.49$ (Fig. 4a and Online Resource 8).

All species exhibited holocentric chromosomes, with large and small chromosomes. *Eleocharis parodii* and *E.*

Table 2 Comparison of nuclear DNA amounts and ploidy levels in species of the *Eleocharis montana* complex

DNA amount/Species	*E. subarticulata*	*E. parodii*	*E. elegans*	*E. contracta*	*E. montana*
2C (pg ± s.d.)	1.570 ± 0.022	1.574 ± 0.006	2.212 ± 0.071	2.772 ± 0.047	4.800 ± 0.076
C*x* (pg)	0.785	0.787	0.553	0.693	0.600
2*n*/2*x*	$2n = 6$	$2n = 2x = 10$	$2n = 4x = 20$	$2n = 4x = 20$	$2n = 8x = 40$

2C DNA content in somatic nuclei; *Cx* hypothetical amount of nuclear DNA in monoploid complements; *pg ± s.d.* average values in picograms for 2C ± standard deviation;

2n diploid chromosome number; *2x* number of monoploid complements based on a basic chromosome number x = 5

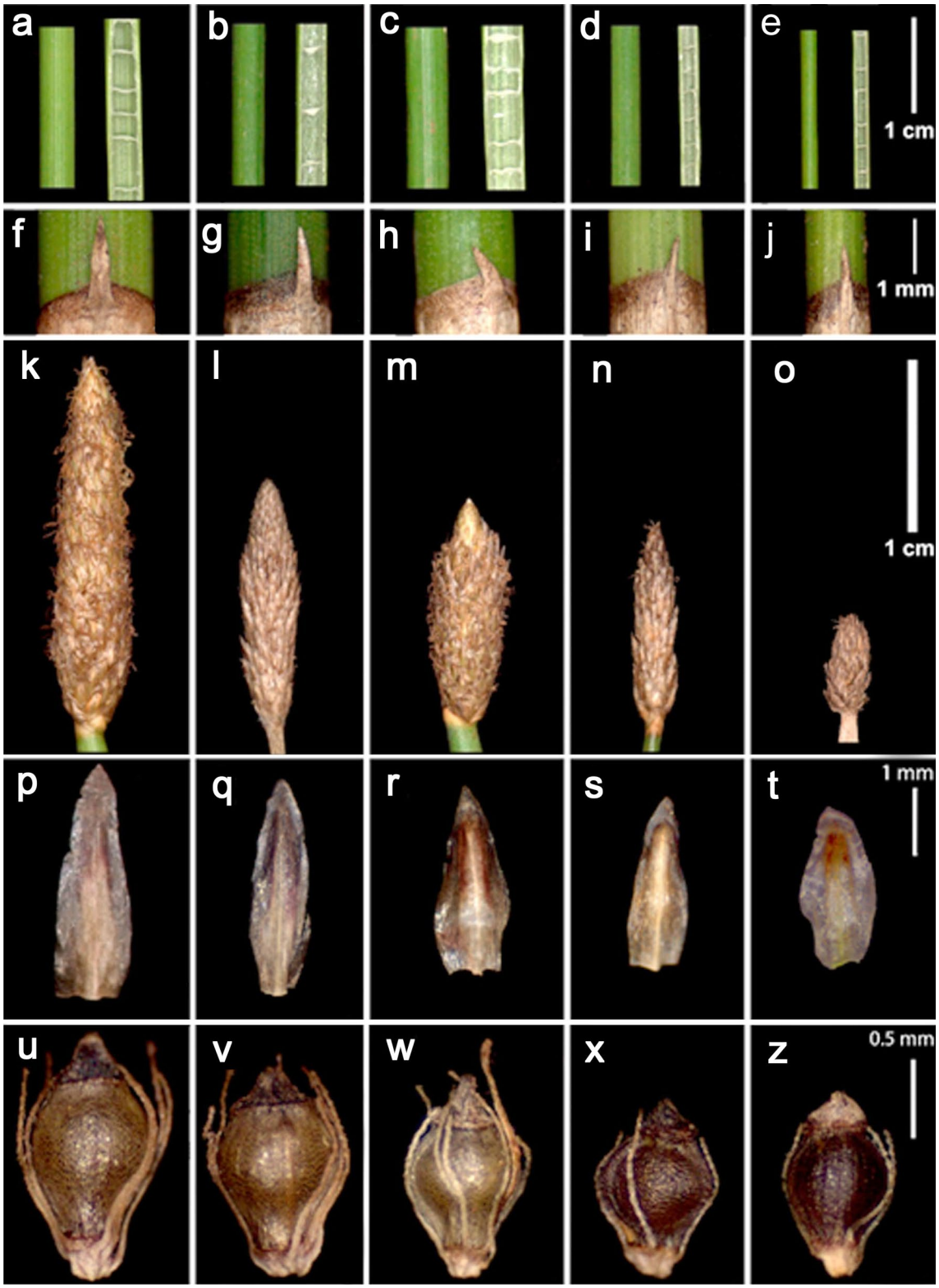

Fig. 2 Phenotype variation inside the *Eleocharis montana* circumscription. The small size trait overlaps with *E. contracta* (Fig. 1). Morphology details of the following are shown: (i) culms (**a–e**) with differences of up to twofold in thickness as well as irregularities in the septa arrangement, being sheath always mucronate (**f–j**); (ii) spikelets (**k–o**) exhibit differences in the number of flowers and are up to threefold variable in the size of mature inflorescences; (iii) scales (**p–t**) are similar in shape but different in their sizes; and (iv) achenes (**u–z**) are similar in shape and perianth bristles, with differences only in the size of mature fruits

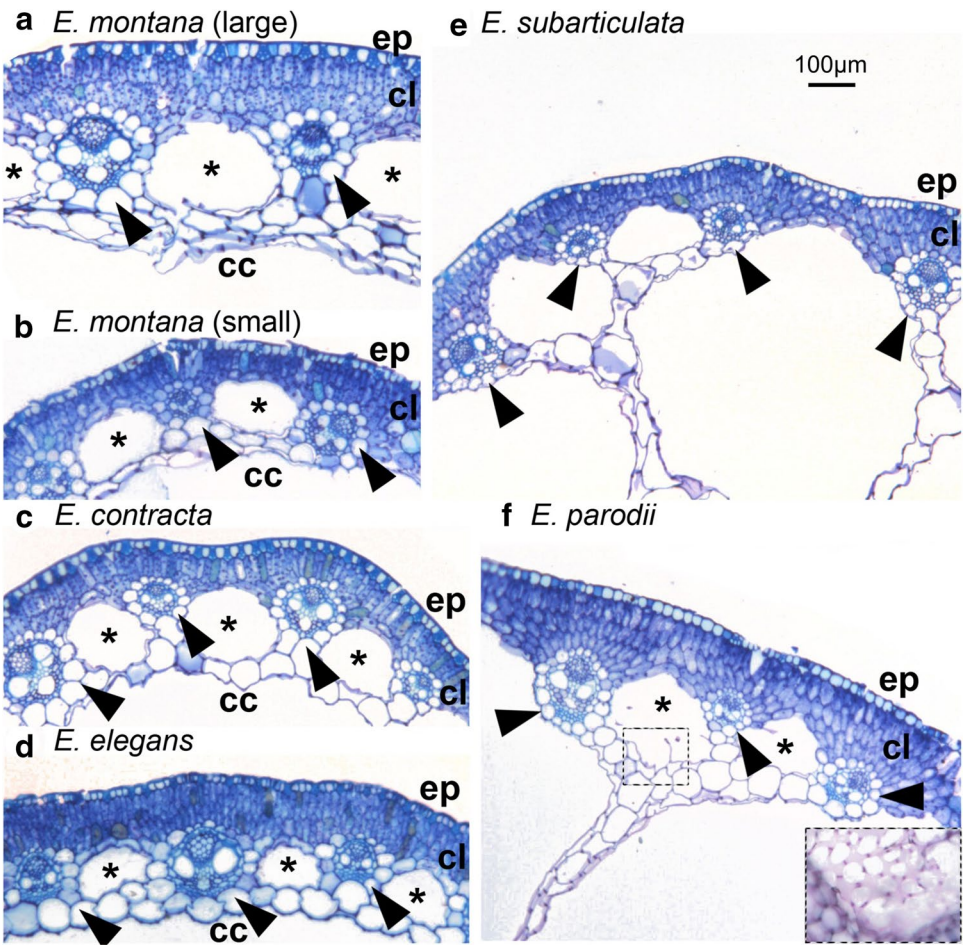

Fig. 3 Transversal sections of *Eleocharis montana*, *E. contracta*, *E. elegans*, *E. subarticulata,* and *E. parodii* culms, stained with 0.05% toluidine blue. The epidermis was uniseriate with some sclerenchimatic fibers (ep). A chlorophytic parenchyma, or chlorenchyma (cl), was present underneath, with either one, two, or three cell layers. Vascular bundles (arrowheads) were present, interspaced with aerenchymatous tissues (*). The latter presented regular cavities in *E. montana* (in both the large and small samples), *E. contracta*, and *E. elegans*. Furthermore, these species presented a large central cavity (cc) in their culms. *Eleocharis subarticulata* and *E. parodii* presented similar features, but without regular aerenchyma cavities or a central cavity. The stellate parenchyma was seen as interspaced with the vascular bundles (inset) only in *E. parodii*. This feature could only be observed in unfixed, unprocessed material

Table 3 Analysis of molecular variance (AMOVA) for 30 individuals of *Eleocharis montana* (16), *E. contracta* (3), *E. elegans* (3), *E. subarticulata* (5), and *E. parodii* (3), using ISSR and REMAP data

VF	DF	SQ	MS	%	*P*
Between populations	7	348.7	49.8	78%	< 0.001
Within populations	22	76.7	3.5	22%	< 0.001
Total	29	425.4		100	

FV variation factor; *DF* degree of freedom; *SQ* sum of square; *MS* mean square; % percentage; and *P* = probability

elegans showed more symmetrical karyotypes, while *E. subarticulata* (derived from symploidy), *E. contracta*, and *E. montana* were asymmetrical. The karyotype of *E. subarticulata* was asymmetrical, with the smallest chromosome having three-fourth the size of the largest, as compared to the symmetrical karyotypes of *E. parodii*. The karyotypes of the tetraploids *E. contracta* and *E. elegans* were also asymmetrical, however, as compared to octaploid *E. montana*, with the largest chromosomes observed to be approximately twice the size of the smallest.

Genome relationships and diversity

The genomes of three species were selected according to their ploidy levels (*E. parodii* (2*n* = 10), *E. elegans* (2*n* = 20), and *E. montana* (2*n* = 40)), and sequenced using Illumina. The raw reads assembled using the 41, 51, and 71 ntd K-mers produced datasets with different features. The assemblages compared to the RepBase, GypsyDB, and NCBI databases revealed both similarities and contrasts among datasets, especially on the repetitive DNA fraction (Fig. 5). First, when we separate the repetitive fraction by classes, there is a homogeneity in the relative quantities (%) regardless of genome size, with predominance of Class I elements (from 72% in *E. elegans* and *E. montana* to 76% in *E. parodii*), followed by Class II, which represented from 18% in *E. parodii* to 20% in *E. elegans* and *E. montana* (Online Resource 9 and Fig. 5a). When we compare them by superfamilies, the relative difference is no more than 15%, except for LINE elements that showed a relative difference of ~ 30% between *E. parodii* and *E. elegans*. The differences between these three genomes were most evident when repetitive families were compared. The most striking differences were for abundances of Retrofit and Athila (with LTR) and L1 (non-LTR)

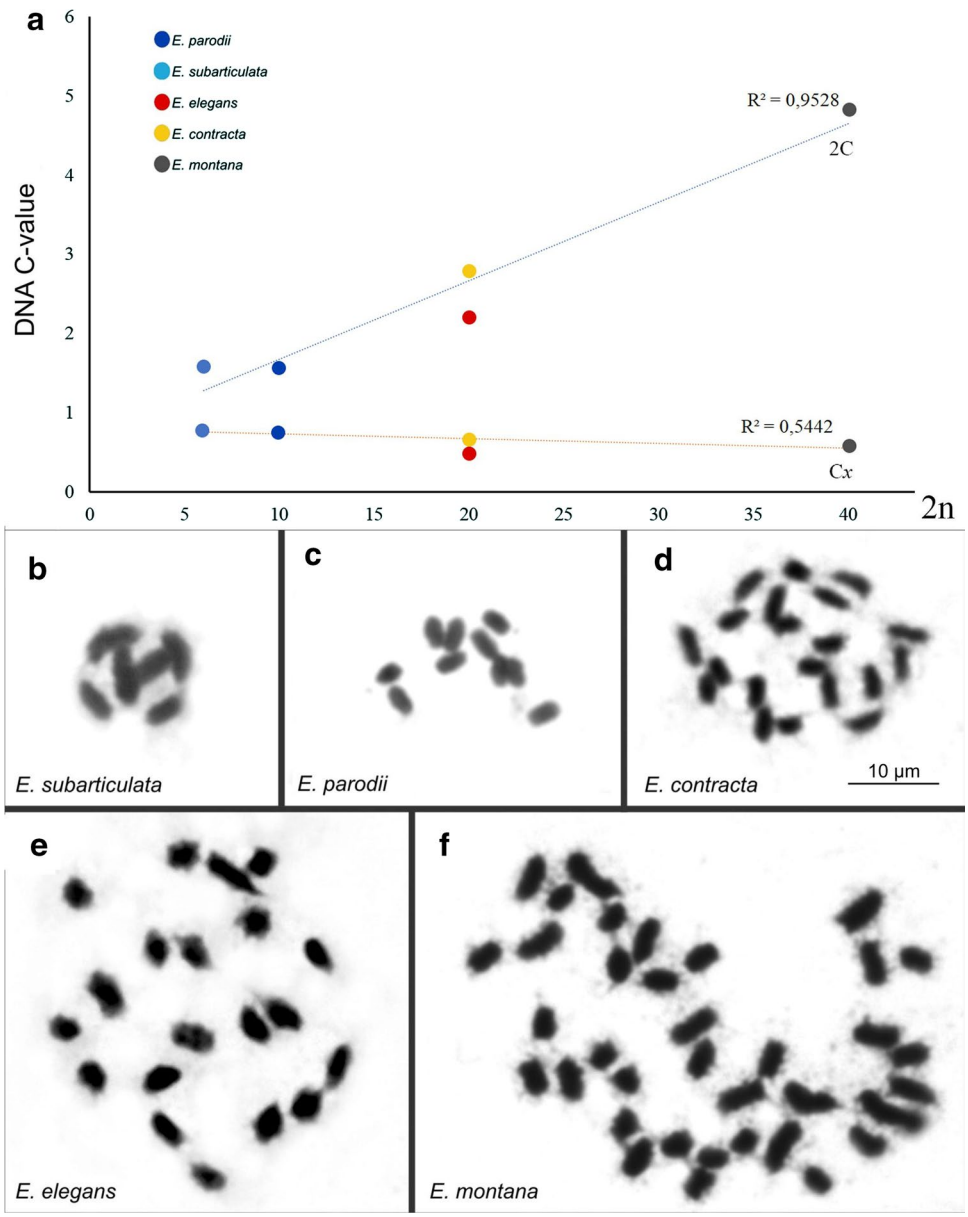

Fig. 4 Distribution of DNA C-values in the *Eleocharis montana* complex species correlated with chromosome numbers. **a** Data of somatic cell DNA (2C) and each monoploid complement (C*x*) appear in picograms and are correlated with chromosome numbers. Values on the right correspond to the Pearson correlation, with $R^2 = 0.95$ for 2*C* and $R^2 = 0.54$ for C*x*. Observe that the 2*C* values have a positive correlation with the ploidy increase, while the C*x* values do not demonstrate such correlation. Giemsa-stained mitotic chromosomes (**b**–**f**) show variation in the chromosome numbers and sizes for *E. subarticulata* $2n = 2x = 6$ (**b**); *E. parodii* $2n = 2x = 10$ (**c**); *E. contracta* $2n = 4x = 20$ (**d**); *E. elegans* $2n = 4x = 20$ (**e**); and *E. montana* $2n = 8x = 40$ (**f**). Note that all species have holocentric chromosomes and the decrease in chromosome sizes is more evident in the dysploid *E. subarticulata* and the octaploid *E. montana*

elements, and rDNA genes (Online Resource 9 and Fig. 5). In general, however, these genomes were not severely contrasting in these repetitive DNA characteristics.

The overview of microsatellite composition obtained with the SSRIT script showed a predominance of 2-mers (dinucleotides) and 3-mers (trinucleotides), with ~90% in *E. parodii*, *E. elegans*, and *E. montana* (Online Resource 10); however, only two 2-mers motifs predominate in the three genomes (AG and GA), with ~13% AG and ~9% GA in these three species. The TA dimer appeared to be well represented in the genomes of *E. parodii* (~38%) and *E. montana* (~27%), whereas this dimer was sparsely present in *E. elegans* (<5%). The analyzed species differed with respect to the 3-mer repeats. The *E. elegans* genome had a lower abundance of 3-mer repeats such as AAT, ATA, and TAA, and a greater accumulation of AAG, AGA, CTT, TAC, and AGT 3-mers in relation to *E. parodii* and *E. montana* genomes. As the oligomers based on GA were predominant in these three genomes (Online Resource 10), the GA_9 oligomer was used as primer for ISSR and REMAP analyses, with reverse transcriptase forward primers of *Copia* and *Gypsy* LTR superfamilies.

The ISSR and REMAP markers produced a total of 98 bands, with 40 polymorphic bands for ISSR, 34 for REMAP-*Copia*, and 31 for REMAP-*Gypsy*. The ANOVA test showed a significant difference ($p < 0.001$) between the species of the *E. montana* complex, with 78% genetic diversity between the species and 22% variance between different populations of each species (Table 3). The dendrogram based on these bands, including a coefficient of correlation of 0.98, grouped samples according to the circumscription of each species, and distanced

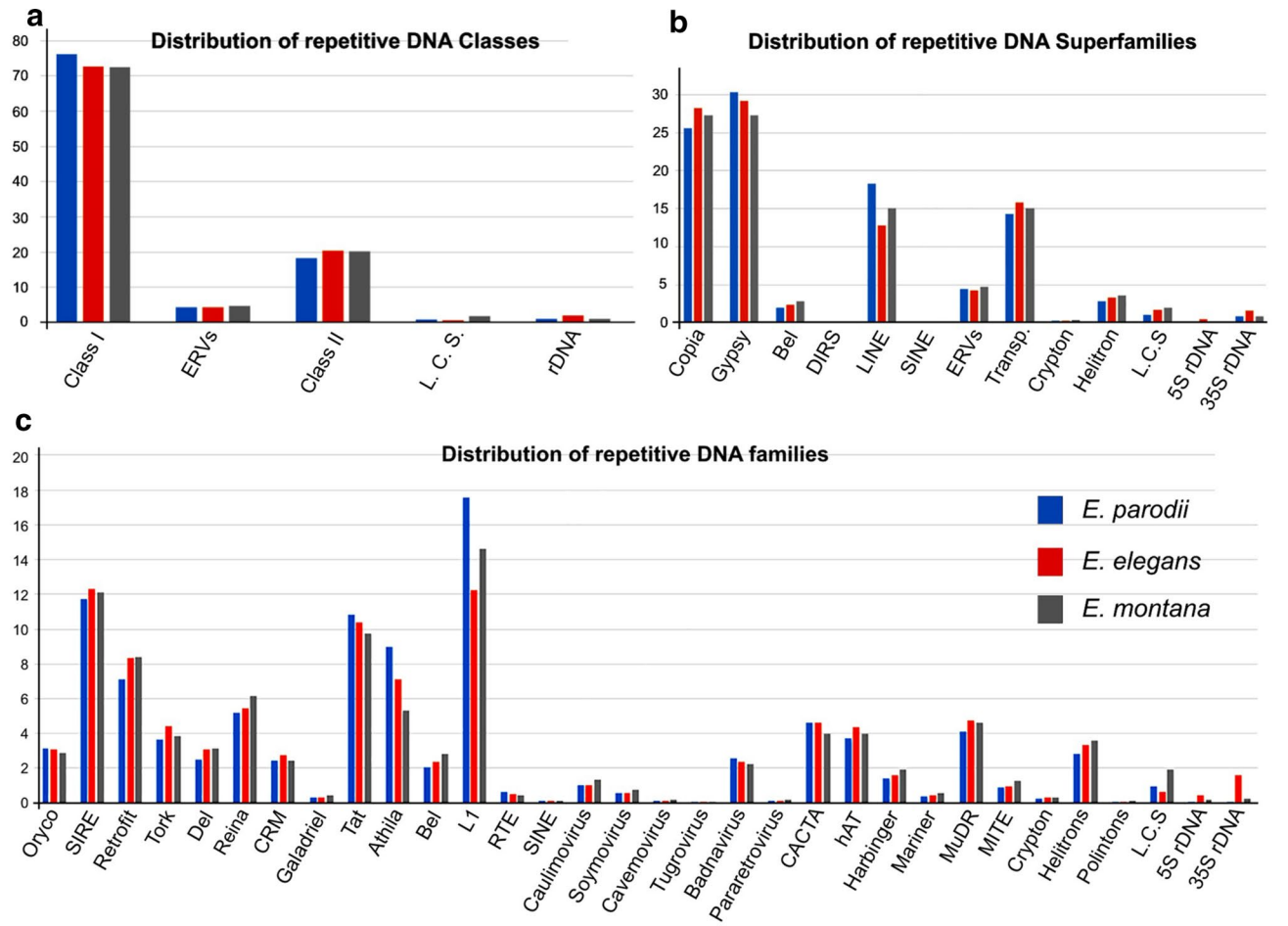

Fig. 5 Relative distribution (%) of repetitive DNA classes in the genomes of *Eleocharis parodii*, *E. elegans,* and *E. montana*, based on low-coverage reads after Illumina sequencing, assembled with the SPAdes tool. Observe the following: **a** Class I transposable elements were most abundant in these data sets; **b** among Class I, *Copia*, *Gypsy*, and LINE elements predominate, while DNA transposons (Class II) accumulate similarly to the LINEs; **c** when observing all lineages, it is possible to note some contrast in the accumulation of Retrofit, Tork, Athila/Tat, L1, SSRs, and rDNA

E. parodii and *E. subarticulata* (diploid and dysploid) from the polyploids *E. elegans*, *E. contracta*, and *E. montana* (Fig. 6).

Data for molecular markers were compared also with a reanalysis of Roalson et al.'s (2010) phylogeny, but restricting it to species of the *E. montana* complex (Online Resource 11), and with a new analysis using sequences from partial 35S rDNA sequences and the partial *pet*N-*psb*M and *trn*C-*ycf*6 chloroplast sequences. This approach made it possible to observe that the genome of *E. acutangula* (Roxb.) Schult. (*E.* subg. *Limnochloa* (P.Beauv. & T.Lestib.) Torr.) appears outside *E. montana* complex clades, whether we have aligned the genes separately (Online Resources 11 and 12) or when all the matrices were concatenated in the Mesquite tool (Online Resource 13). Inside the complex, two clusters predominated: the first was composed of *E. contracta* and *E. montana* and the second with *E. parodii* and *E. subarticulata. Eleocharis elegans* appeared as a distinct subclade of *E. parodii* and *E. subarticulata*. In fact, these two species, which are the most related morphologically and, in some cases, almost indifferentiable (*E. contracta* with $2n = 20$ and *E. montana* with $2n = 40$), appeared together in the phylogeny, similar to what was observed using the ISSR and REMAP markers.

GISH supporting the hybridization history

In order to test for instances of natural hybridization throughout the evolutionary history of the *E. montana* complex, the diploid genome of *E. parodii* with $2n = 10$ was used as a probe against all karyotypes. This probe hybridized very well to half of the chromosomes of *E. elegans* with $2n = 20$ (Fig. 7a–c), *E. contracta* with $2n = 20$ (Fig. 7d–f), and *E. montana* with $2n = 40$ (Fig. 7g–i), with very low brightness signals on the other half. When the genome of *E. contracta*, the other tetraploid with $2n = 20$, was tested as a probe, all chromosomes of *E. montana* appeared to be hybridized in a homogeneous manner (Fig. 7j–l). The genome of *E. elegans*, a tetraploid with

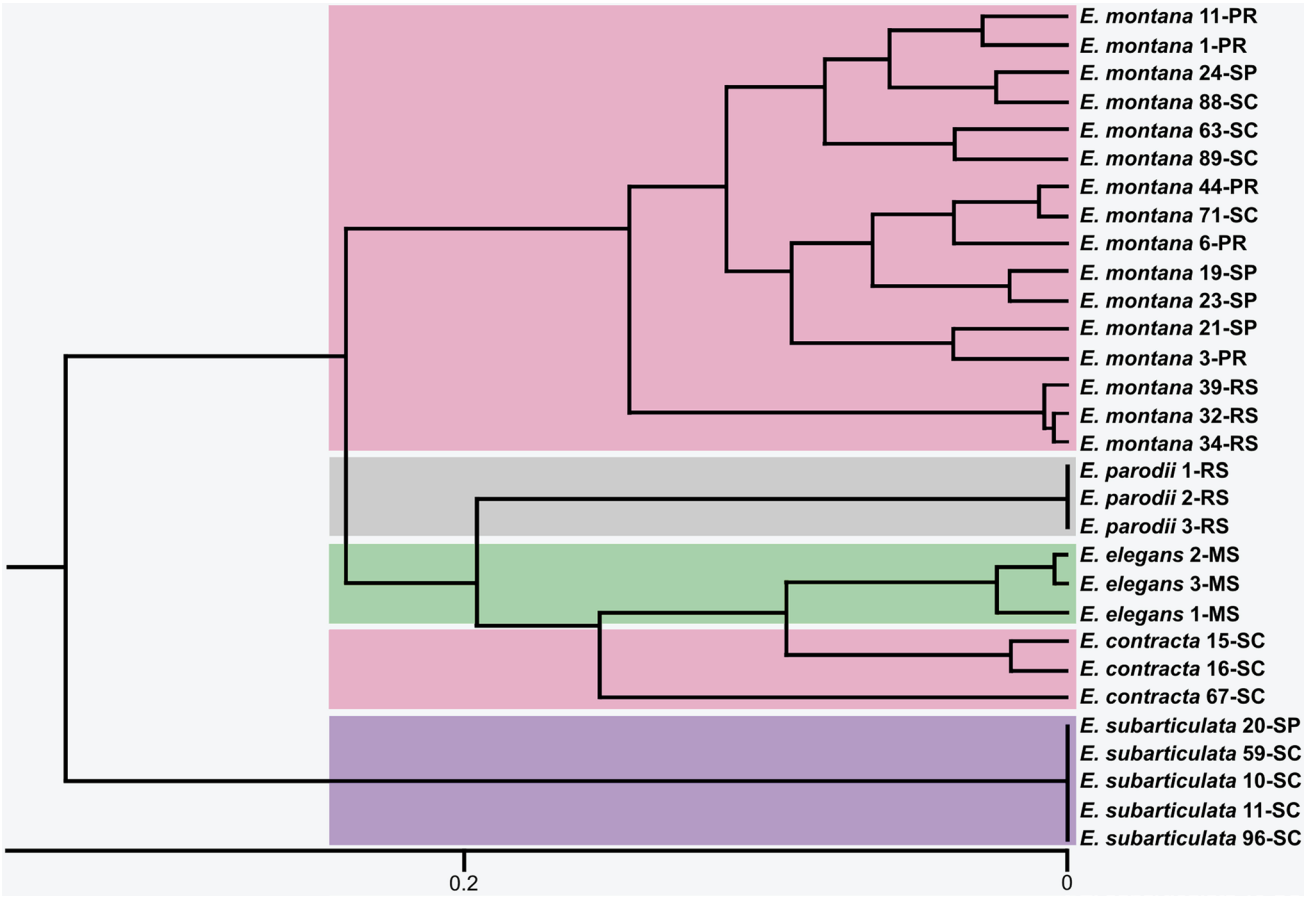

Fig. 6 Dendrogram based in the bands produced by ISSR and REMAP markers with a coefficient of correlation of 0.98. Samples appear grouped according to the circumscription of each species. Observe that *Eleocharis parodii* (diploid) appears in the base of *E. elegans* and *E. contracta* (tetraploid species), and close to *E. montana* (octaploid). This genetic approximation plot is compatible with the re-evaluation of the Roalson-based (2010) phylogeny (see Online Resource 11)

$2n=20$, was also used as a probe in GISH against karyotypes of all species. Herein, half of the chromosomes of *E. contracta* (Fig. 8a–c) and *E. montana* (Fig. 8d–f) hybridized strongly, with weak signals in the other half. The GISH using genomes of *E. contracta* or *E. montana* as the probe showed hybridization signals in all chromosomes of *E. elegans* (Fig. 8g–l). *Eleocharis subarticulata* was not used as a probe because the symploid karyotype with $2n=6$ and a multivalent ring at meiosis did not suggest a progenitor role to species with $2n=20$ and 40, at least with the symploid karyotype found so far.

Discussion

Natural hybridization and polyploidy played an important role in the evolution of the *Eleocharis montana* complex

The South American species of the *E. montana* complex are organized in two subseries according to the presence of truncated sheath apex and a well-developed mucron (*E. elegans*, *E. contracta*, and *E. montana*, in subseries *Truncatae*), and those with an underdeveloped or missing mucron (*E. subarticulata* and *E. parodii*, in subseries *Eleocharis*) (González-Elizondo and Peterson 1997). This division is also followed by culm anatomy that distinguishes species of subseries *Truncatae* from *Eleocharis*, especially by the presence or absence of regular aerenchyma cavities despite some reports that consider culm anatomy conserved in the genus *Eleocharis* (Eiten 1969; Ueno et al. 1989; Rocha and Martins 2011; Krähmer 2016).

When all the morphological features are analyzed separately, it seems evident that there is overlap in diagnostic features, which can hinder distinguishing these species (González-Elizondo and Peterson 1997; Trevisan 2009). *Eleocharis elegans, E. subarticulata*, and *E. parodii* seem to be similar on the stylobases of achenes, although features such as spikelet shape, sheath, and culms, as well as the morphological matrix analysis using the Mesquite software,

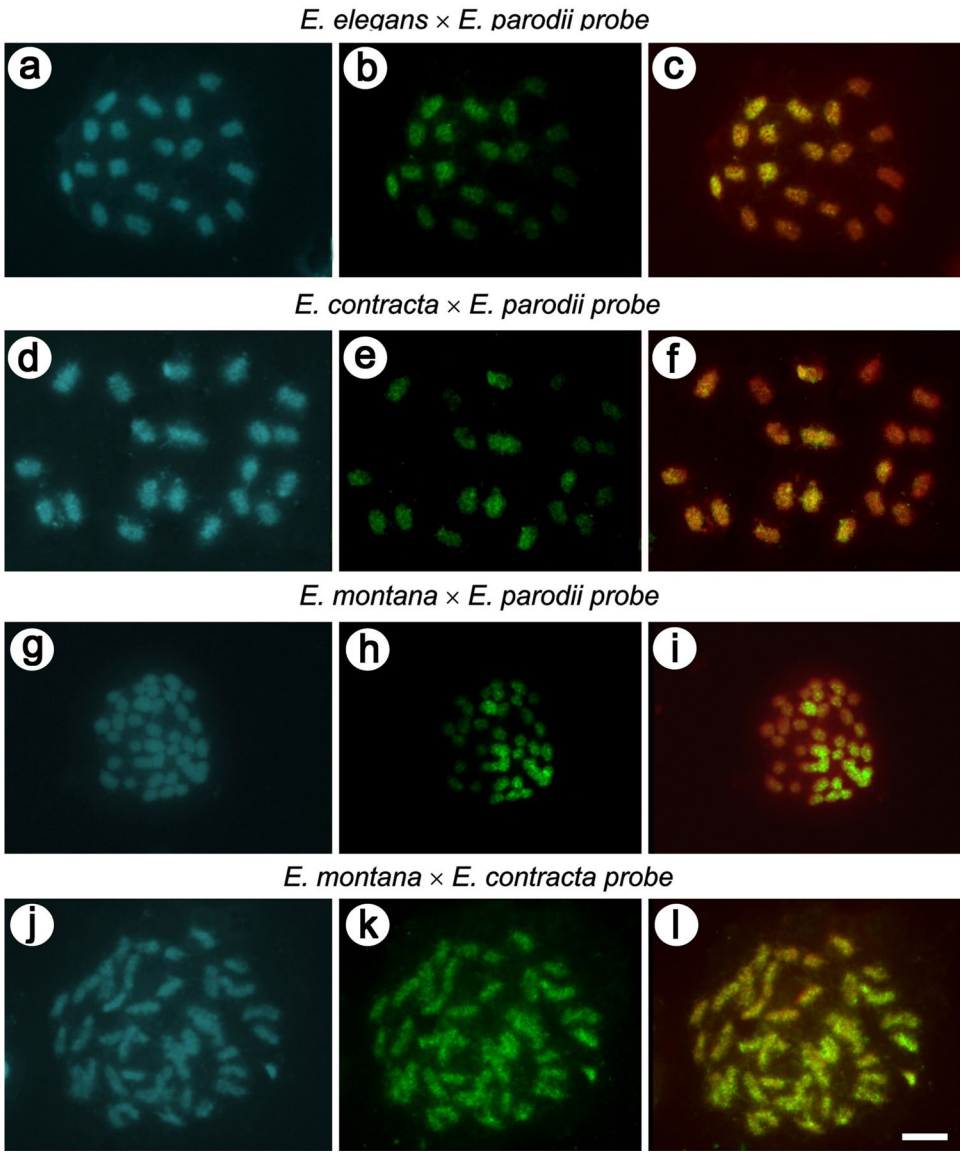

Fig. 7 GISH using the *Eleocharis parodii* ($2n = 10$) genomic probe against *E. elegans* (**a**–**c**), *E. contracta* (**d**–**f**), and *E. montana* (**g**–**i**) mitotic chromosomes. Note that this probe hybridized strongly to half of the chromosomes of each species. When the *E. montana* chromosomes were hybridized with the genomic probe of *E. contracta* ($2n = 20$) (**j**–**l**), all chromosomes were labeled, indicating an intimate relationship between these two genomes. The chromosomes were counterstained with DAPI (blue). The GISH probe was detected with avidin-FITC (green) and, in the merged images, the DAPI was pseudo-red

have placed *E. elegans* close to *E. contracta* and *E. montana*. These last species are very similar, differing only in structure sizes, with *E. contracta* appearing as a small version of *E. montana*, such as reported by Trevisan (2009). The overlap of morpho-anatomical features observed among species of the *E. montana* complex, together with high phenotype plasticity of *E. montana*, and the close relationship with *E. contracta*, point to the hybridization involving this group. However, we cannot recognize typical characteristics of the progenitor *E. parodii* in the hybrids.

The REMAP and ISSR markers, and the genetic diversity approach using rDNA and chloroplast sequences, all supported the morpho-anatomical and taxonomical studies (see González-Elizondo and Peterson 1997; Trevisan 2009; Roalson et al. 2010), because they grouped *E. contracta* with *E. montana*. In fact, these two species are morphologically very similar, and in some cases almost indifferentiable. In the second clade, *E. parodii* was linked to *E. subarticulata*, and *E. elegans* appeared slightly farther from them. Still, if we compare these relationships with the chromosome sizes and the molecular markers, it is clear that, in addition to the polyploidy, there were increases in the karyotype asymmetry and a greater activity of repetitive DNA families in the octaploid *E. montana*, in comparison with the species with lower ploidy levels.

Flutuations in DNA C-values and on karyotypes diversity are associated with polyploidy

Over 8000 plant species have had their DNA C-value estimated (http://data.kew.org/cvalues/), and polyploidy has been seen to be an important mechanism for increasing nuclear DNA content in plants (e.g., Gitaí et al. 2014). Variations in plants DNA C-values can also occur due to

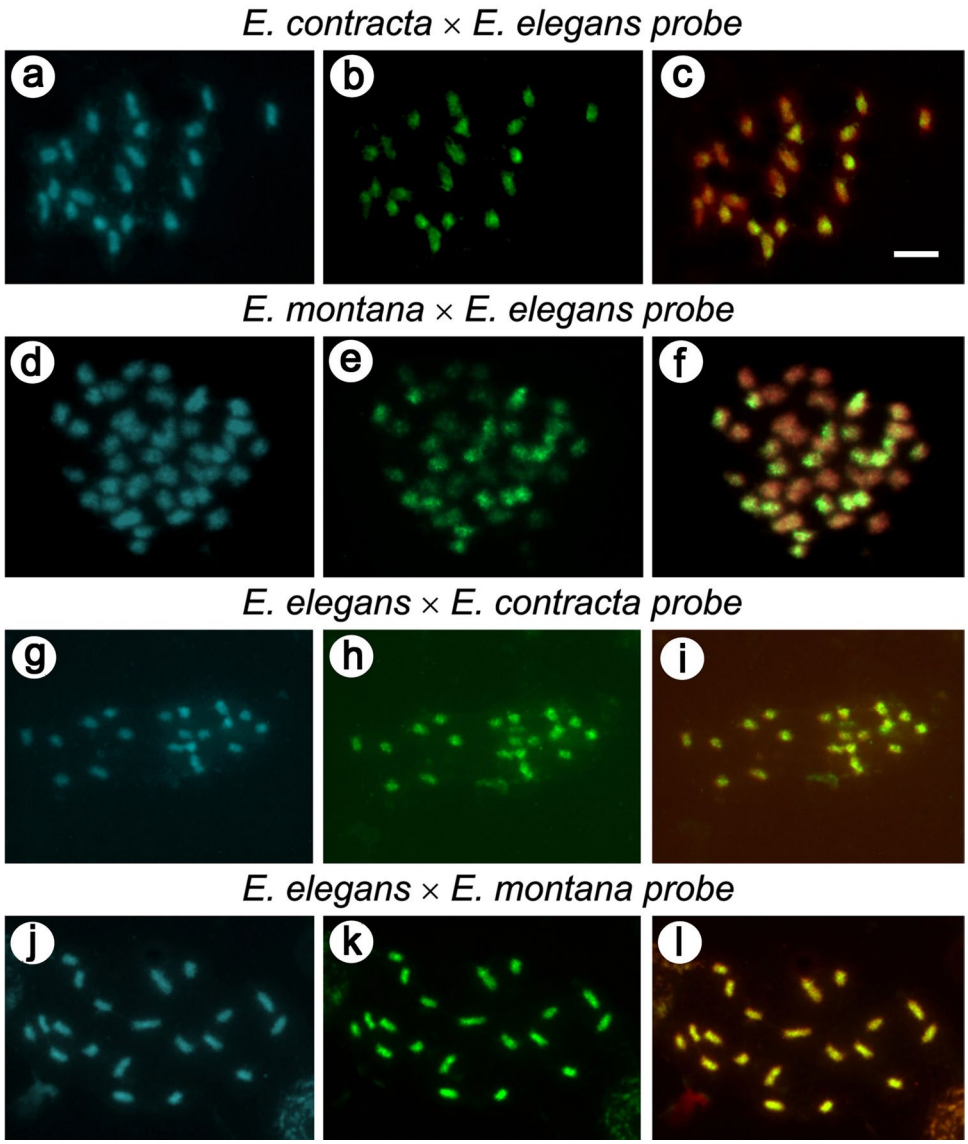

Fig. 8 GISH of the *Eleocharis elegans* (2n = 20) genomic probe was hybridized against the chromosomes of *E. contracta* and *E. montana* (**a**–**f**). Observe that half of the karyotype presents strong hybridization signals. The genomic probes of *E. contracta* and *E. montana* were hybridized against the chromosomes of *E. elegans*, respectively (**g**–**l**). In both cases, all *E. elegans* chromosomes were hybridized. This suggests that *E. elegans*, *E. contracta*, and *E. montana* share a common progenitor. The chromosomes were counterstained with DAPI (blue), and the GISH probe was detected with avidin-FITC (green). In the merged images, the DAPI appears pseudo-red

other events, such as accumulation or elimination of repetitive DNA portion and also chromosome rearrangements (Heslop-Harrison and Schwarzacher 2011; Tenaillon et al. 2011; Souza et al. 2018). There is evidence of DNA C-value changes associated with dysploidy between populations of *Eleocharis maculosa* with $2n = 10$ ($2C = 1$ pg) and $2n = 6$ with $2C = 0.86$ pg (Souza et al. 2018); however, when we compared the diploidy *E. parodii* ($2n = 10$) with the dysploid *E. subarticulata* ($2n = 6$), both with $2C = 1.57$ pg, we cannot suggest considerable changes on DNA amount as a result of structural chromosomal changes.

In general, the $2C$ values increased proportionally to the higher ploidy levels inside the *E. montana* complex, with ~ 70% between genomes with $2n = 10$ and 40, and ~ 50% between $2n = 20$ and 40. This increase is in accordance with the report of Souza et al. (2018) that showed a difference of 75% in the $2C$ value between species with $2n = 10$ and 40, of 50% between species with $2n = 20$ and 30, and 65% between species with $2n = 20$ and 40. When we expanded the comparison between *Eleocharis*, ranges from 0.84 to 18 pg (Zedek et al. 2010), and other Cyperaceae, such as *Carex* (0.3–2.3 pg), *Eriophorum* (0.75–1.3 pg), *Scirpus* (0.8–1.0 pg), and *Cyperus*, which ranges from 0.9 to 2.75 pg (see Bennett and Leitch 2012), we could note that the differences in the $2C$ values were not as broad as in *Eleocharis*. From what we have seen so far, these genera present more dysploids than polyploids (Roalson 2008). Although DNA C-value fluctuations in dysploid and polyploid *Eleocharis* species are evident in our study, more DNA C-value studies in a larger number of Cyperaceae genera are needed to confirm this trend.

Allopolyploid origins and migration from the hybridization zone

Austral South America seems to have been a hotspot for species diversification for *Eleocharis*. The first comprehensive study of this topic was published by Da Silva et al. (2017) in the complex *Tenuissimae* (*E. ramboana* R.Trevis. & Boldrini, *E. viridans* Kük. ex Osten, and *E. niederleinii* Boeckeler), where the authors showed an expansion of polyploid and dysploid hybrids that emerged from this region. Our evidence using morpho-anatomical data, molecular markers, and DNA sequences drew our attention to the possibility of a hybrid origin of *E. elegans*, *E. contracta* and *E. montana*, arisen from the progenitors *E. parodii* and *E. subarticulata*. However, *E. subarticulata* is a dysploid with $2n=6$ (Da Silva et al. 2005) and with meiosis incompatible to the generation of the species analyzed here. The only diploid tested as progenitor was *E. parodii* ($2n=10$), first as one of the ancestors of *E. contracta* and *E. montana* and afterward as a parental species to *E. elegans*.

The use of GISH was efficient for this ancestral origin investigation, as well as to detect hybrids in other plant groups, such as in Solanaceae (Chase et al. 2003), Liliaceae (Marasek et al. 2004), and Leguminosae (Marques et al. 2018), and earlier in *Eleocharis* (Da Silva et al. 2017). The *E. parodii* probe produced hybridization signals in half of the chromosomes of *E. contracta*, *E. montana*, and *E. elegans*, which was confirmed by reverse GISH, using polyploid genome probes against each other and also against the diploid. Given this, our suggestion is that *E. parodii* participated as a progenitor of *E. elegans* and *E. contracta* in an independent way and, subsequently, *E. contracta* underwent autopolyploidy, giving rise to the octaploid cytotype of *E. montana*.

Based on intermediate chromosome numbers, hybrids in *Eleocharis* "subseries Palustris" (= Subsect. *Eleocharis*), including subspecies of *E. palustris* (L.) Roem. & Schult. and *E. uniglumis* Schult., have been reported by Strandhede (1965, 1966). In other reports, hybrids have been reported between *E. compressa* and *E. erythropoda* (Catling 1994), *E. cellulosa* and *E. interstincta* (Košnar et al. 2010), and *E. cellulosa* and *E. quadrangulata* (Rosen and Reid 2015). Additionally, this holds true in other Cyperaceae, such as in *Carex* (Catling et al. 1989), *Schoenoplectus*

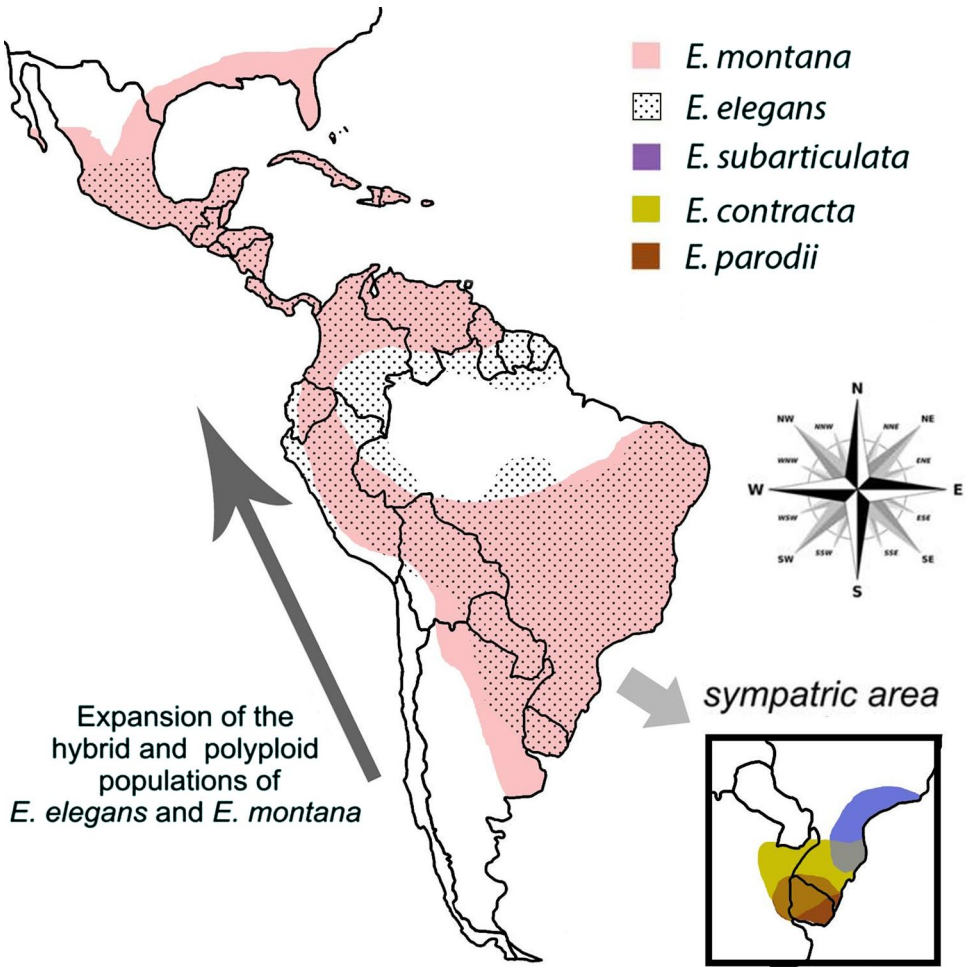

Fig. 9 Distribution of the *Eleocharis montana* complex species in the American continents. The map shows the path of the polyploids (*E. montana* and *E. elegans*) from the diversification region in the southern hemisphere toward the north. All of the species occur in the sympatry area. Observe that two species appear in North and Central America. These two species have overlapping morphological features with *E. contracta*

(Fay et al. 2003), and *Scirpus* (Yang et al. 2009). However, only two reports show the species relationship based on hybridization, polyploidy, and disploidy in the evolution of the *Eleocharis* clades: the study of Da Silva et al. (2017) of the series *Tenuissimae* and the present study of the *E. montana* complex.

Although this comparative study has been comprehensive, there were some difficulties in obtaining high-population representativeness, since species such as *E. parodii* and *E. contracta* are difficult to find in the field. Even though we were effective at identifying one of the progenitors, the other was not found. Due to the small chance of the other progenitor being of African origin, a South American progenitor species may be rare, extinct, or belonging to another clade. In this sense, *Eleocharis guaglianoniana* J.P.R.Ferreira, Silv. Venturi & R.Trevis. could be the lost progenitor, because it is morphologically close to *E. subarticulata*. However, this species belongs to the other clade and is very rare in Southern Brazil (Ferreira et al. 2015). Notwithstanding, this does not disqualify *E. parodii* as one progenitor. According to Roalson et al. (2010), there is a close relationship between *E. ravenelii* Britton (from Central America) and *E. contracta* and *E. montana*, but *E. ravenelii* is a rare species, collected only a few times. As *E. ravenelii* occurs in a large disjunction of the diversification center of the group (Austral South America; Fig. 9), additional data are necessary to prove this hypothesis.

Concluding remarks

The literature attests that natural hybridization has contributed extensively to angiosperm diversity (Soltis and Soltis 2009). Hybrids and polyploids tend to occupy novel habitats and landscapes, sometimes overlapping with the habitats of diploids and making the diploid progenitors less abundant, even at their center of diversification. The distribution map (Fig. 9) shows that *E. parodii* and *E. subarticulata* occur in a restricted area of Austral South America, which overlaps with the occurrence area of the polyploids *E. elegans* and *E. montana* (see also Trevisan 2009; WCSP 2014). These last two species expanded their occurrence areas from the hybridization zone in Austral South America to part of North America. Our data prove that the *E. montana* complex species follow the general profile of the subgenus *Eleocharis* about the diversity in the chromosome numbers and DNA amount, and that allopolyploidy and dysploidy events have been key factors in the evolutionary history of this complex.

Acknowledgements The authors thank the Brazilian agencies FINEP, Fundação Araucária, CNPq, CAPES, and ProPPG-UEL for their financial support. We thank also the Department of Structural Biology, Molecular, and Genetics from Universidade Estadual de Ponta Grossa for technical support. The authors declare no conflict of interest within this article. A.L.L. Vanzela and R. Trevisan thank CNPq for the productivity scholarship (numbers 309902/2018-5 and 313306/2018-4, respectively).

Authors contribution L. Johnen, T.B. de Souza, and D. M. Rocha performed all the experiments, wrote and corrected the manuscript. M. S. González-Elizondo and R. Trevisan were responsible for species identifications, support for morphological analyses and for manuscript corrections. S.R. Chaluvadi and J.L. Bennetzen performed the genomic sequencing, supported the bioinformatic analysis, and edited the manuscript. A.L.L. Vanzela designed the study, checked the data analyses, and organized, wrote, and corrected the manuscript.

Information on Electronic Supplementary Material

Supplementary materials include list of species with samples localities and maps, images of achenes morphological analysis, anatomical sections of culms, dendrograms and DNA sequences, and comparative tables and graphs of composition of the repetitive DNA families. All these information complements the results presented in the main text.

Online Resource 1. Data for the *Eleocharis montana* complex sampled in this study.
Online Resource 2. Geographic localization of the collected populations of *Eleocharis parodii*, *E. contracta*, *E. elegans*, *E. montana*, and *E. subarticulata* from Brazilian regions.
Online Resource 3. Sequence alignment used in genetic relationship analysis.
Online Resource 4. Species differentiation using achene shapes and borders.
Online Resource 5. Comparison of morphological features using a distance matrix by the UPGMA method.
Online Resource 6. Measurements of diagnostic morphological structures of *Eleocharis montana.*
Online Resource 7. Culm anatomies of *Eleocharis montana*, *E. elegans, E. contracta*, *E. subarticulata*, and *E. parodii*, stained with 0.05% toluidine blue.
Online Resource 8. DNA C-value estimates for the *Eleocharis montana* complex.
Online Resource 9. Distribution of repetitive DNA elements on the assembled genomes of *Eleocharis parodii* ($2n=10$), *E. elegans* ($2n=20$) and *E. montana* ($2n=40$).
Online Resource 10. In silico microsatellite scanning in three *Eleocharis* datasets.
Online Resource 11. Phylogeny based on Roalson et al. (2010), using the Brazilian *Eleocharis montana* complex species (Subgenus *Eleocharis*), plus *E. acutangula* (subg. *Limnochloa*) as an outgroup.
Online Resource 12. Comparison of trees using partial 35S rDNA and chloroplast (*pet*N-*psb*M and *trn*C-*ycf*6) sequences.
Online Resource 13. Dendrogram concatenating data of partial 35S rDNA and chloroplast genes, molecular markers and morphological features using the Mesquite tool.

References

Bennett MD, Leitch IJ (2012) Angiosperm DNA *C*-values database (release 6.0, Dec. 2012). Available at: https://cvalues.science.kew.org/

Bureš P, Zedek F (2014) Holokinetic drive: centromere drive in chromosomes without centromeres. Evolution 68:2412–2420. https://doi.org/10.1111/evo.12437

Catling PM (1994) *Eleocharis compressa* × *Eleocharis erythropoda*, a new natural hybrid spike rush from Ontario. Canad J Bot 72:837–842. https://doi.org/10.1139/b94-108

Catling PM, Reznicek AA, Denford K (1989) *Carex lacustris* × *C. trichocarpa* (Cyperaceae), a new natural hybrid. Canad J Bot 67:790–795. https://doi.org/10.1139/b89-106

Chase MW, Knapp S, Cox AV, Clarkson JJ, Butsko Y, Joseph J, Savolainen V, Parokonny AS (2003) Molecular systematics, GISH and the origin of hybrid taxa in *Nicotiana* (Solanaceae). Ann Bot (Oxford) 92:107–127. https://doi.org/10.1093/aob/mcg087

Da Silva CRM, González-Elizondo MS, Vanzela ALL (2005) Reduction of chromosome number in *Eleocharis subarticulata* (Cyperaceae) by multiple translocations. Bot J Linn Soc 149:457–464. https://doi.org/10.1111/j.1095-8339.2005.00449.x

Da Silva CRM, Trevisan R, González-Elizondo MS, Ferreira JM, Vanzela ALL (2010) Karyotypic diversification and its contribution to the taxonomy of *Eleocharis* (Cyperaceae) from Brazil. Austral J Bot 58:49–60. https://doi.org/10.1071/BT09185

Da Silva CRM, Souza TB, Trevisan R, González-Elizondo MS, Torezan JMD, de Souza RF, Vanzela ALL (2017) Genome differentiation, natural hybridisation and taxonomic relationships among *Eleocharis viridans*, *E. niederleinii* and *E. ramboana* (Cyperaceae). Austral Syst Bot 30:183–195. https://doi.org/10.1071/SB17002

Dar TH, Raina SN, Goel S (2017) Cytogenetic and molecular evidences revealing genomic changes after autopolyploidization: a case study of synthetic autotetraploid *Phlox drummondii* hook. Physiol Molec Biol Pl 23:641–650. https://doi.org/10.1007/s12298-017-0445-8

Del Pozo JC, Ramirez-Parra E (2015) Whole genome duplications in plants: an overview from *Arabdopsis*. J Exp Bot 66:6991–7003. https://doi.org/10.1093/jxb/erv432

Doležel J, Greilhuber J, Suda J (2007) Estimation of nuclear DNA content in plants using flow cytometry. Nat Protoc 2:2233–2244. https://doi.org/10.1038/nprot.2007.310

Doyle JJ, Doyle JL (1987) A rapid DNA isolation procedure for small quantities of fresh leaf tissue. Phytochem Bull 19:11–15

Eiten LT (1969) The vegetative anatomy of *Eleocharis interstincta* (Vahl) Roem. and Schult. Arq Bot Estado São Paulo 4:187–228

Escudero M, Hahn M, Hipp AL (2018) RAD-seq linkage mapping and patterns of segregation distortion in sedges: meiosis as a driver of karyotypic evolution in organisms with holocentric chromosomes. J Evol Biol 31:833–843. https://doi.org/10.1111/jeb.13267

Fay MF, Cowan RS, Simpson DA (2003) Hybridisation between *Schoenoplectus tabernaemontani* and *S. triqueter* (Cyperaceae) in the British Isles. Watsonia 24:433–442

Fazekas AJ, Kesanakuri PR, Burgess KS, Percy DM, Grahm SW, Barrett SCH, Newmaster SG, Hajibabaei M, Husband BC (2009) Are plant species inherently harder to discriminate than animal species using DNA barcoding markers? Molec Ecol Resources 9:130–139. https://doi.org/10.1111/j.1755-0998.2009.02652.x

Ferreira JPR, Venturi S, Trevisan R (2015) *Eleocharis guaglianoniana* (Cyperaceae), a new species from southern Brazil. J Torrey Bot Soc 142:186–192. https://doi.org/10.3159/TORREY-D-14-0078

Gerrits PO, Smid L (1983) A new, less toxic polymerization system for the embedding of soft tissues in glycol methacrylate and subsequent preparing of serial sections. J Microscop 132:81–85. https://doi.org/10.1111/j.1365-2818.1983.tb04711.x

Gitaí J, Paule J, Zizka G, Schulte K, Benko-Iseppon AM (2014) Chromosome numbers and DNA content in Bromeliaceae: additional data and critical review. Bot J Linn Soc 176:349–368. https://doi.org/10.1111/boj.12211

Goetghebeur P (1998) Cyperaceae. In: Kubitzki K (ed) Flowering plants monocotyledons, vol. 29. Springer, Berlin, pp 141–190

González-Elizondo MS, Peterson PM (1997) A classification of and key to the supraspecific taxa in *Eleocharis* (Cyperaceae). Taxon 46:433–449. https://doi.org/10.2307/1224386

González-Elizondo MS, Tena-Flores JA (2000) *Eleocharis* (Cyperaceae) in the New World. In: Wilson KL, Morrison DA (eds) Monocots: systematics and evolution. CSIRO, Sidney, pp 637–643

Heslop-Harrison JS, Schwarzacher T (2011) Organisation of the plant genome in chromosomes. Pl J 66:18–33. https://doi.org/10.1111/j.1365-313X.2011.04544.x

Hinchliff CE, Lliully Aguilar AE, Carey T, Roalson EH (2010) The origins of *Eleocharis* (Cyperaceae) and the phylogenetic position of *Websteria*, *Egleria*, and *Chillania*. Taxon 59:709–719

Kalendar R, Schulman AH (2006) IRAP and REMAP for retrotransposon-based genotyping and fingerprinting. Nat Protoc 1:2478–2484. https://doi.org/10.1038/nprot.2006.377

Kerbs B, Ressler J, Kelly JK, Mort ME, Santos-Guerra A, Gibson MJS, Caujapé-Castells J, Crawford DJ (2017) The potential role of hybridization in diversification and speciation in an insular plant lineage: insights from synthetic interspecific hybrids. AoB PLANTS 9:1–12. https://doi.org/10.1093/aobpla/plx043

Košnar J, Košnar J, Herbstová M, Macek P, Rejmánková E, Štech M (2010) Natural hybridization in tropical spikerushes of subgenus (Cyperaceae): Evidence from morphology and DNA markers. Amer J Bot 97:1229–1240

Krähmer H (2016) Aerenchyma within the stem. In: Krähmer H (ed), Atlas of weed mapping. John Wiley & Sons, Hoboken, pp 194–214

Llorens C, Muñoz-Pomer A, Bernad L, Botella H, Moya A (2009) Network dynamics of eukaryotic LTR retroelements beyond phylogenetic trees. Biol Direct 4:41

Luceño M, Guerra M (1996) Numerical variations in species exhibiting holocentric chromosomes: a nomenclatural proposal. Caryologia 49:301–309. https://doi.org/10.1080/00087114.1996.10797374

Marasek A, Hasterok R, Wiejacha K, Orlikowska T (2004) Determination by GISH and FISH of hybrid status in *Lilium*. Hereditas 140:1–7. https://doi.org/10.1111/j.1601-5223.2004.01721.x

Marques A, Moraes L, Aparecida dos Santos M, Costa I, Costa L, Nunes T, Melo N, Simon MF, Leitch AR, Almeida C, Souza G (2018) Origin and parental genome characterization of the allotetraploid *Stylosanthes scabra* Vogel (Papilionoideae, Leguminosae), an important legume pasture crop. Ann Bot (Oxford) 122:1143–1159. https://doi.org/10.1093/aob/mcy113

Queiroz K (2007) Species concepts and species delimitation. Syst Biol 56:879–886. https://doi.org/10.1080/10635150701701083

Rambaut A (2007) FigTree, a graphical viewer of phylogenetic trees. Available at: http://tree.bio.ed.ac.uk/software/figtree

Ribeiro T, Buddenhagen CE, Thomas WW, Souza G, Pedrosa-Harand A (2018) Are holocentrics doomed to change? Limited chromosome number variation in *Rhynchospora* Vahl (Cyperaceae). Protoplasma 255:263–272. https://doi.org/10.1007/s00709-017-1154-4

Roalson EH (2008) A synopsis of chromosome number variation in the Cyperaceae. Bot Rev 74:209–393. https://doi.org/10.1007/s12229-008-9011-y

Roalson EH, Hinchliff CE, Trevisan R, da Silva CRM (2010) Phylogenetic relationships in *Eleocharis* (Cyperaceae): C4 photosynthesis origins and patterns of diversification in the spikerushes. Syst Bot 35:257–271. https://doi.org/10.1600/036364410791638270

Rocha DC, Martins D (2011) Adaptações morfoanatômicas de Cyperaceae ao ambiente aquático. Pl Danin 29:7–15

Rosen DJ, Reid C (2015) *Eleocharis*×*inaequilatera* (Cyperaceae), a new hybrid spikerush from the coastal plain of Louisiana and Texas. Phytoneuron 23:1–5

Soltis PS, Soltis DE (2009) The role of hybridization in plant speciation. Annual Rev Pl Biol 60:561–588. https://doi.org/10.1146/annurev.arplant.043008.092039

Souza TB, Chaluvadi SR, Johnen L, Marques A, González-Elizondo MS, Bennetzen JL, Vanzela ALL (2018) Analysis of retrotransposon abundance, diversity and distribution in holocentric *Eleocharis* (Cyperaceae) genomes. Ann Bot (Oxford) 122:279–290. https://doi.org/10.1093/aob/mcy066

Strandhede SO (1965) Chromosome studies in *Eleocharis*, subser. Palustres. III. Observations on Western European taxa. Opera Bot 9:1–86

Strandhede SO (1966) Morphologic variation and taxonomy in European *Eleocharis*, subser. Palustres. Opera Bot 10:1–187

Tenaillon MI, Hufford MB, Gaut BS, Ross-Ibarra J (2011) Genome size and transposable element content as determined by high-throughput sequencing in maize and *Zea luxurians*. Genome Biol Evol 3:219–229. https://doi.org/10.1093/gbe/evr008

Trevisan R (2009) *Eleocharis* (Cyperaceae) na Região Sul do Brasil. PhD Thesis, Federal University of Rio Grande do Sul, Rio Grande do Sul

Ueno O, Samejima M, Koyama T (1989) Distribution and evolution of C4 syndrome in *Eleocharis*, a sedge group inhabiting wet and aquatic environments, based on culm anatomy and carbon isotope ratios. Ann Bot (Oxford) 64:425–438. https://doi.org/10.1093/oxfordjournals.aob.a087861

WCSP: World Checklist of Selected Plant Families (version Sep 2014). In: Roskov Y, Abucay L, Orrell T, Nicolson D, Kunze T, Flann C. Bailly N, Kirk P, Bourgoin T, DeWalt RE, Decock W, De Wever A (eds) Species 2000 and ITIS Catalogue of Life, 2015 Annual Checklist. Naturalis, Leiden. Available at: www.catalogueoflife.org/col

Whitney KD, Ahern JR, Campbell LG, Albert LP, King MS (2010) Patterns of hybridization in plants. Perspect Pl Ecol 12:175–182. https://doi.org/10.1016/j.ppees.2010.02.002

Yang M, Zhou Y, Zhu Q, Lu F, Wang Y, Chen J, Wu Q, Zhang W (2009) AFLP markers in the detection of *Scirpus*×*mariqueter* (CYPERACEAE) hybrid in China. Aquat Bot 91:298–302. https://doi.org/10.1016/j.aquabot.2009.08.005

Yano O, Katsuyama T, Tsubota H, Hoshino T (2004) Molecular phylogeny of Japanese *Eleocharis* (Cyperaceae) based on ITS sequence data, and chromosomal evolution. Int J Pl Res 117:409–419. https://doi.org/10.1007/s10265-004-0173-3

Yano O, Tanaka N, Ito Y (2016) Molecular evidence for a natural hybrid between *Isolepis crassiuscula* and *Isolepis lenticularis* (Cyperaceae) in New Zealand. New Zealand J Bot 54:433–445. https://doi.org/10.1080/0028825X.2016.1205106

Zedek F, Šmerda J, Šmarda P, Bureš P (2010) Correlated evolution of LTR retrotransposons and genome size in the genus *Eleocharis*. BMC Pl Biol 10:265. https://doi.org/10.1186/1471-2229-10-265